

# Retraction Hooks of Different Lengths for Maxillary Whole Arch Distalization with Miniscrew Anchorage: A Finite Element Analysis

Vanichaya Tangsumroengvong<sup>1</sup>, Virush Patanaporn<sup>2</sup>, Chaiy Rungsiyakul<sup>3</sup>

<sup>1</sup>Graduate student, Division of Orthodontics, Faculty of Dentistry, Chiang Mai University

<sup>2</sup>Department of Orthodontics and Pediatric, Faculty of Dentistry, Chiang Mai University

<sup>3</sup>Department of Mechanical Engineering, Faculty of Engineering, Chiang Mai University

CM Dent J 2021; 42(1) : 125-138

Received: 20 April, 2020

Revised: 14 May, 2020

Accepted: 22 May, 2020

## Abstract

**Objectives:** To evaluate the von Mises stress distribution in the periodontal ligament and the displacement pattern of maxillary whole arch distalization applied to retraction hooks of different lengths with miniscrew anchorage and to determine the optimal length of retraction hook, using a finite element method.

**Methods:** A finite element model of maxillary teeth with periodontal ligament and alveolar bone was constructed. The miniscrews were placed bilaterally 6 mm above the buccal cemento-enamel junction at the modified infrazygomatic crest site. The distalization force of 200 g was applied to 0-, 2-, 4-, 6-, 8-mm-length retraction hooks located between the lateral incisors and canines. The stress distribution in the periodontal ligament and the displacement of the teeth were analyzed. The optimal length of retraction hook for maximal distal movement of the maxillary whole arch along the occlusal plane was investigated.

**Results:** The von Mises stress in the anterior teeth was greater than in the posterior teeth with all hook lengths. When using the short hooks, the areas of high stress were in the lateral incisor, canine and second molar. When using the long hooks, the areas of high stress were in the anterior teeth. With the 0-mm and 2-mm lengths, the anterior teeth were extruded and tipped palatally; the posterior teeth were intruded and tipped distally. With the 4-mm length, all maxillary teeth were distalized along the occlusal plane with minimal movement in the vertical direction. The anterior teeth were slightly tipped labially; the posterior teeth were slightly tipped distally. With the 6-mm and

---

Corresponding Author:

**Visush Patanaporn**

Clinical Professor, Department of Orthodontics and Pediatric Dentistry, Faculty of Dentistry, Chiang Mai University, Chiang Mai 50200, Thailand

E-mail: [vr167420@hotmail.com](mailto:vr167420@hotmail.com)

8-mm lengths, the anterior teeth were intruded and tipped labially; the posterior teeth were extruded and tipped distally. The optimal length in this study was found to be 4 mm.

**Conclusions:** Different lengths of retraction hooks resulted in different patterns of stress distribution in the PDL and in different patterns of displacement of the maxillary teeth in whole arch distalization. The optimal length of retraction hook was 4 mm for maximal distal movement of the maxillary whole arch along the occlusal plane.

**Keywords:** whole arch distalization, en-masse distalization, finite element, retraction hook

## Introduction

Non-extraction treatment of Class II malocclusion requires maxillary dentition distalization, mandibular dentition mesialization, or a combination of both.<sup>(1,2)</sup> Distalization can be divided into sequential distalization and en-masse distalization. In the sequential distalization, initially the first and second molars are distalized by open-coil spring, then the premolars and then the anterior teeth. This method can cause proclination of the anterior teeth and distal tipping of the molars during distalization.<sup>(3,4)</sup> En-masse distalization is achieved by distalizing all of the anterior and posterior teeth at the same time, as one rigid block, using miniscrew anchorage.<sup>(1,5-8)</sup> Although this method may reduce the overall treatment time, it may increase the risk of root resorption since the applied magnitude of force is larger than that of the sequential distalization.<sup>(7)</sup>

Miniscrew implant placement locations for maxillary dentition distalization are varied.<sup>(9,10)</sup> The placement locations include the midpalatal or paramedian areas of the palate,<sup>(11)</sup> the buccal or palatal interradicular areas,<sup>(6,7,9)</sup> and the infrazygomatic crest.<sup>(8)</sup> The most ideal safe zone for placing miniscrews for distalization of the maxillary dentition is the region between the maxillary first and second molar in the infrazygomatic crest area,<sup>(9)</sup> which is called the "Modified infrazygomatic crest site." (Modified IZC)<sup>(12,13)</sup> This site provides thick cortical

bone and fewer problems with root proximity than in the interradicular areas.<sup>(8,9)</sup>

Each study and case report conducted previously applied different loading forces for whole arch distalization, ranging from 200 to 300 g.<sup>(5-8,12,14,15)</sup> Most of them, however, used a force magnitude of about 200 g and found no side effect in terms of root resorption and periodontitis.<sup>(5-7,12)</sup> Therefore, the force magnitude of 200 g will be chosen for this study.

The relationship between the line of action of the applied force and the center of resistance (CRes) defines the type of tooth movement.<sup>(4)</sup> Force passing through the CRes causes translation; force passing off-center causes rotation or tipping.<sup>(16)</sup> Clinically, it is difficult to accurately determine the line of force passing through the CRes of the maxillary dentition. Moving the line of force close to the CRes by applying the force to a different retraction hook lengths can cause more translational movement rather than applying the force at the bracket level.<sup>(3)</sup> Jeong *et al.*<sup>(32)</sup> reported that the CRes of the maxillary dentition in their finite element model constructed from Nissin commercial tooth model was 13.5 mm. apically and 12.0 mm. posteriorly to the incisal edge of the maxillary central incisors. As our study will also use Nissin dental model, we will choose this location as the CRes of our finite element model.

The finite element method is a contemporary

research tool in orthodontics for measuring structural stress and for movement analyses.<sup>(17,18)</sup> It is a numerical stress analysis which can be used to describe the stress situation within the periodontal ligament (PDL) and surrounding alveolar bone.<sup>(19)</sup> This method has become popular since it is completely non-invasive, very accurate and it is based on the mathematical properties of the structures.<sup>(18)</sup> The purposes of this study were to use the finite element method to evaluate the pattern of stress distribution in the PDL and the tooth displacement pattern of maxillary whole arch distalization relative to force vectors applied to retraction hooks of different lengths and to determine the optimal length of retraction hook for maximal distal movement of the maxillary whole arch along the occlusal plane, when using miniscrew anchorage placed at the modified IZC.

## Materials and methods

All maxillary teeth of a commercial model (Model-i21FE-400C; Nissin Dental Products, Kyoto, Japan) based on the average tooth dimensions of Asian adults with normal occlusion were scanned via 3-D laser scanning to make digital tooth images.<sup>(20-25)</sup> The solid model, including all maxillary teeth, PDL and maxillary bone was constructed and assembled using SolidWorks software (Dassault Systèmes Americas, Waltham, Mass., USA). The maxillary bone consisted of cancellous bone with 1.0 mm thickness of cortical bone. The alveolar crest was formed following the curvature of the cemento-enamel junction (CEJ), 1 mm apical to the CEJ.<sup>(24,26)</sup> The thickness of the PDL was assumed to be a uniform 0.2 mm. The brackets were modeled with slot dimensions of a 0.018 x 0.025 inches and attached to the midpoint of the facial axis of the crown and completely connected to each tooth. The main archwire was modeled as a stainless-steel wire with dimensions of 0.017 x 0.025 inches, and it was assumed that there was no play and no friction

between the brackets and the archwire. Retraction hooks were modeled using 0.036 inch crimpable hook stainless steel and located bilaterally between the lateral incisors and canines. The miniscrew position was simulated 6 mm above the buccal CEJ between the maxillary first and second molars at the position of the modified IZC, as proposed by Lin.<sup>(12)</sup>

The properties of all materials were those used in previously conducted finite element studies (Table 1).<sup>(27-33)</sup> All materials were assigned isoparametric, homogeneous, linear, elastic properties, excepting the PDL, which was defined as having non-linear elasticity. Ogden model property values were assigned to describe the non-linear elastic stress-strain behavior of the PDL (Table 2).<sup>(34)</sup>

The constructed finite element model was meshed into 148,914 nodes and 651,810 elements. The teeth, PDL and alveolar bone were constructed into tetrahedron elements. The brackets, hooks, and archwire were constructed into hexahedron elements. The interactions between teeth were tie contact with no friction. The boundary conditions were defined at the top and back surface of the maxillary bone.

**Table 1** Material properties of dentin, cortical bone, cancellous bone and stainless steel required within the FE model.<sup>(27-33)</sup>

Material	Young's modulus (MPa)	Poisson's ratio
Dentin	19600	0.3
Cortical bone	13700	0.26
Cancellous bone	1370	0.3
Stainless steel	200000	0.3

**Table 2** Coefficients of the third order Ogden model property values describing non-linear elasticity of PDL.<sup>(34)</sup>

i	$\mu_i$	$a_i$	$D_i$
1	-24.4237106	1.99994222	4.87164332
2	15.8966494	3.99994113	0.00000000
3	8.56953079	-2.00005453	0.00000000

The orientation of this model was established with the x axis representing the mesio-distal direction of the anterior teeth and the bucco-palatal direction of the posterior teeth. The y axis represented the supero-inferior direction. The z axis represented the antero-posterior direction, which is the labio-palatal direction of the anterior teeth and the mesio-distal direction of the posterior teeth. +X represents the left side of model, in the right quadrant, +x represents the mesial direction of movement of the anterior teeth and the palatal direction of movement of the posterior teeth. In the left quadrant, +x represents the distal direction of movement of the anterior teeth and the buccal direction of movement of the posterior teeth. +Y values were defined as the inferior or apical direction and +z values were defined as the labial direction of the anterior teeth or the mesial direction of the posterior teeth (Figure 1).

A distalization force vector of 200 g was applied from the miniscrew to the retraction hooks of 0-mm, 2-mm, 4-mm, 6-mm, and 8-mm lengths (Figure 2). The location of CRes was defined same as the location described by Jeong *et al.*<sup>(31)</sup> The displacement patterns of the teeth, produced by the force vectors resulting from using each hook length, were calculat-

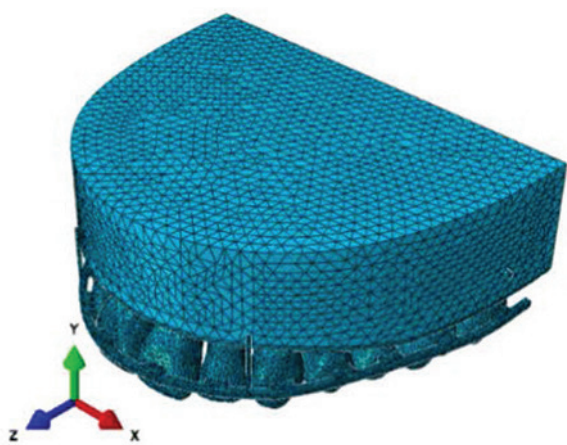


**Figure 1** The orientation of the model. X axis: (+) left, (-) right direction; y axis: (+) superior; (-) inferior direction; z axis: (+) anterior; (-) posterior direction.

ed in the x, y, and z axes. The midpoints of the incisal edges of the central and lateral incisors, the cusp tip of the canine, the buccal cusp tips of the premolars, the mesio-buccal cusp tips of the molars, and the root apices of each tooth were used as reference points to evaluate the displacement of the teeth. The Abaqus software (Dassault Systèmes Americas) was used to calculate and visualize the PDL von Mises stress distribution and tooth displacement patterns for the whole arch distalization of all maxillary teeth.

## Results

Von Mises stress distribution in PDL and tooth displacement patterns of the right and left quadrants were assumed to be the same because the point of application and angle of force direction were the

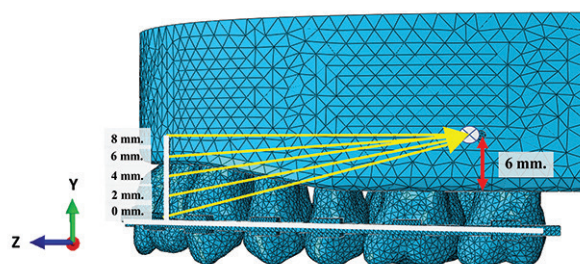


**Figure 2** Schematic force diagram and miniscrew position. Forces (200 g) were applied from the miniscrew to different vertical positions of the retraction hook: 0 mm, 2 mm, 4 mm, 6 mm and 8 mm. located between the lateral incisor and canine. The location of miniscrew was simulated at 6 mm above the buccal CEJ between the first and second molar.

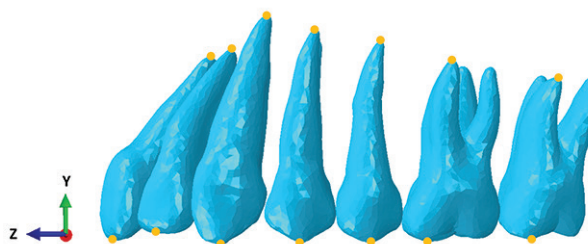


**Figure 3** The reference points of teeth are represented as yellow dots for the assessment of tooth displacement.

same. Therefore, only the left quadrant is shown in these results, for clarity and to eliminate superimposition of the right and left quadrants.

### Von Mises stress distribution in PDL

The von Mises stress distribution in the PDL was calculated in  $\text{N/mm}^2$  (MegaPascals or MPa). The color-coded map of von Mises stress distribution in the PDL with all hook lengths is shown in Figure 4. The levels of stress are shown in the map, in which red represents the areas of maximum stress and dark blue represents the areas of minimum stress.

The stress produced when using 0-mm retraction hooks was greatly concentrated in the canine and the distal root of the second molar. The highest stress value was in the cervical third of the canine ( $2.939 \times 10^{-4}$  MPa). The lowest stress value was in the

apical third of the central incisor ( $3.751 \times 10^{-9}$  MPa) (Figure 4A).

The stress produced when using 2-mm retraction hooks was greatly concentrated in the lateral incisor, canine and the distal root of the second molar. The highest stress value was in the cervical third of the canine ( $4.465 \times 10^{-4}$  MPa). The lowest stress value was in the apical third of the central incisor ( $6.286 \times 10^{-9}$  MPa) (Figure 4B). The distribution patterns of the above two hook lengths are nearly the same pattern.

With the 4-mm length of retraction hook, the highest stress value was in the apical third of the lateral incisor ( $4.162 \times 10^{-4}$  MPa). The high stress was also found in the second molar but lower than with the 0-mm and 2-mm hooks. The lowest stress value was in the apical third of the first premolar

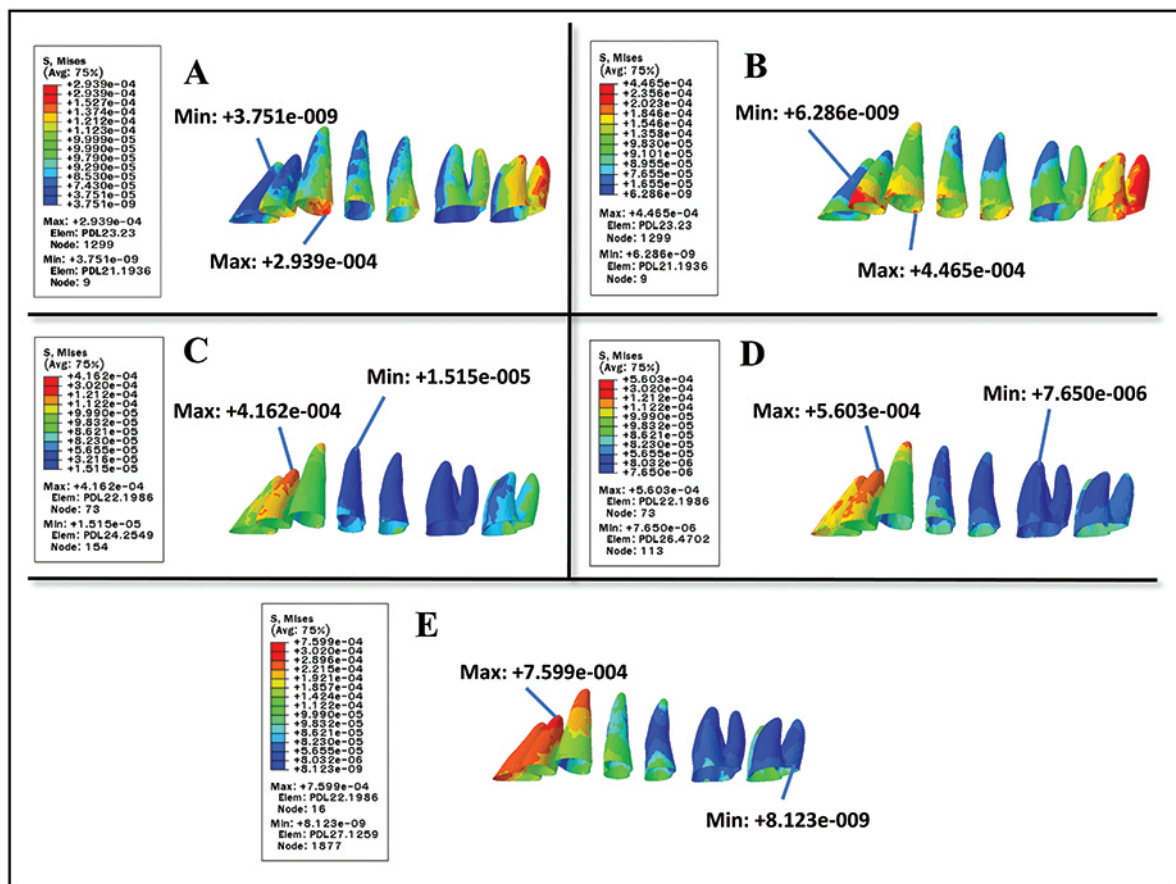


**Figure 4** Color-coded map of von Mises stress distribution in the left maxillary quadrant PDL. The areas of maximum and minimum stress are indicated. A) 0-mm, B) 2-mm, C) 4-mm, D) 6-mm, E) 8-mm lengths

( $1.515 \times 10^{-5}$  MPa) (Figure 4C).

With the 6-mm length of retraction hook, the areas of high stress were in the apical third of the central incisor, lateral incisor and canine. The highest stress value was in the apical third of the lateral incisor ( $5.603 \times 10^{-4}$  MPa). The lowest stress value was in the apical third of the first molar ( $7.650 \times 10^{-6}$  MPa) (Figure 4D).

With the 8-mm length of retraction hook, the areas of high stress were nearly the same pattern with the 6-mm length, but the stress was more concentrated. The highest stress value was in the apical third of the lateral incisor ( $7.599 \times 10^{-4}$  MPa). The lowest stress value was in the cervical third of the second molar ( $8.123 \times 10^{-9}$  MPa) (Figure 4E).

#### **Displacement of all maxillary teeth**

The displacement patterns of all maxillary teeth with each length of retraction hook are shown in Figure 4. The translucent yellow tooth images show the positions of the teeth before applying the force, and the blue tooth images show the displaced positions afterwards. The directions of the arrows adjacent to the teeth represent the directions of the tooth movement. The length and color of the arrows represent the distance of the tooth movement. With all lengths of retraction hooks, the amounts of initial tooth movement in the anterior segment were larger than in the posterior segment.

With the retraction hook lengths of 0 mm (bracket slot level) and 2 mm, palatal crown tipping and extrusion of the anterior teeth were observed. The posterior tooth movement was distal tipping and intrusion (Figure 5A & B). In the occlusal view, all teeth moved in the posterior direction with the anterior teeth moving palatally and the posterior teeth moving distally. The crowns of the posterior teeth tipped slightly buccally (Figure 6A & B).

With the retraction hook length of 4 mm, both crowns and roots of the anterior teeth moved

palatally and slightly intruded. The root apices displaced palatally more than the crowns. The crowns of posterior teeth moved distally. The premolars were slightly extruded, but the molars were slightly intruded (Figure 5C). In the occlusal view, all teeth still moved in the posterior direction but, in contrast to the situation with 0-mm and 2-mm hooks, the crowns of the posterior teeth tipped slightly palatally (Figure 6C).

With the retraction hook length of 6 mm and 8 mm, the direction of anterior tooth movement changed from palatal crown tipping to labial crown tipping. The anterior segment of archwire was raised upward, resulting in anterior teeth proclination and intrusion. The posterior teeth tipped slightly distally and extruded (Figure 5D & E). In the occlusal view, the crowns of the anterior teeth tipped labially and the root apices tipped palatally. The crowns of the posterior teeth tended to tip palatally to a greater extent than with the 4-mm hook (Figure 6D & E).

#### **Optimal length of retraction hook**

The optimal length of retraction hook in this study was 4 mm. The anterior and posterior teeth moved distally along the occlusal plane with minimal vertical movement and tipping.

## **Discussion**

This finite element study of maxillary whole arch distalization demonstrates that applying distalization force to different lengths of retraction hooks resulted in different patterns of stress distribution in the PDL and in different patterns of displacement of the maxillary teeth. We also found that the optimal length of retraction hook that produced closed to distal translation movement of the maxillary whole arch was 4 mm.

Applying distalization force to the retraction hook, the initial movement was mainly observed at the anterior teeth as proved by FEM. The force

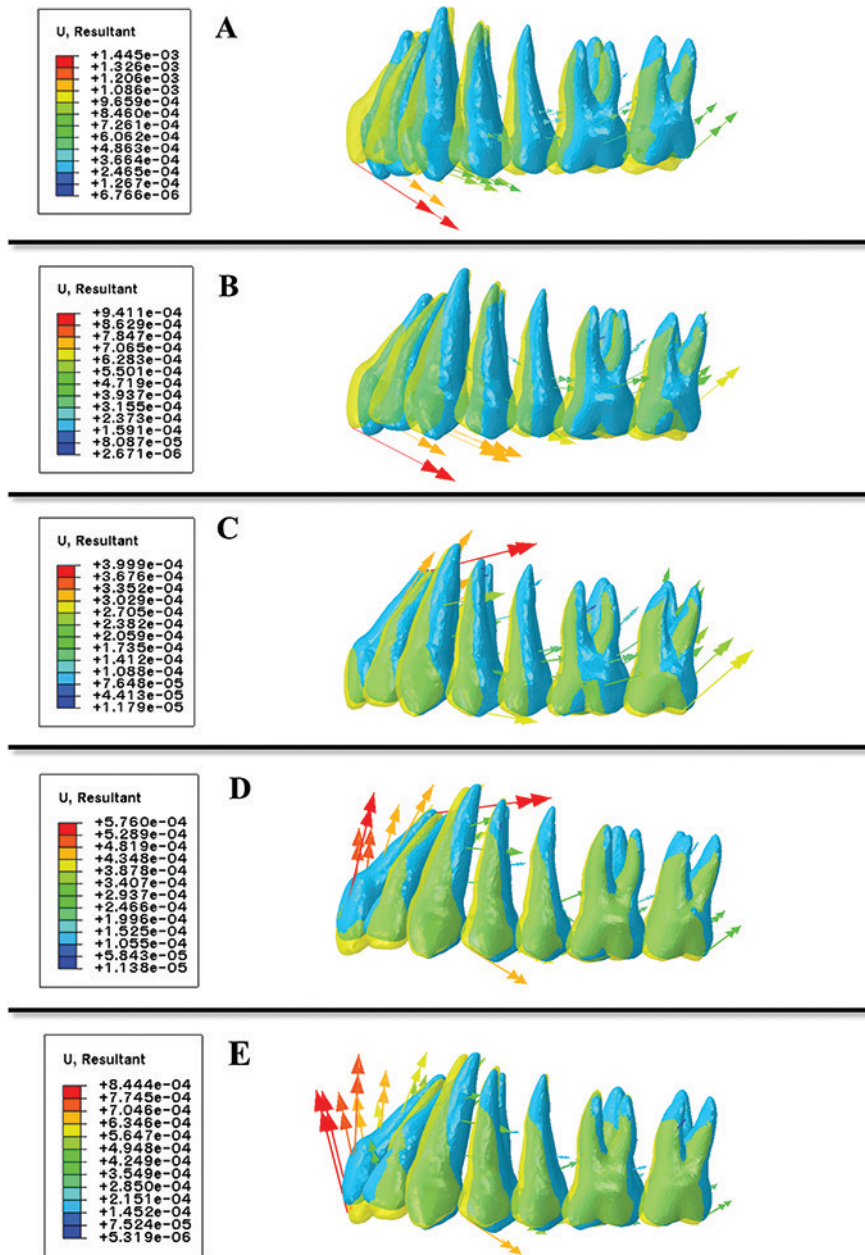


**Figure 5** Displacement of the left maxillary teeth indicated by superimposition of before (yellow) and after (blue) application of the distalization force. The direction of tooth movement indicated by the colored arrows. The length and color of the arrows represent the distance of the tooth movement. Long red arrows indicate large amounts of displacement; short blue arrows indicate small amounts of displacement. A) 0-mm., B) 2-mm., C) 4-mm., D) 6-mm., E) 8-mm. lengths

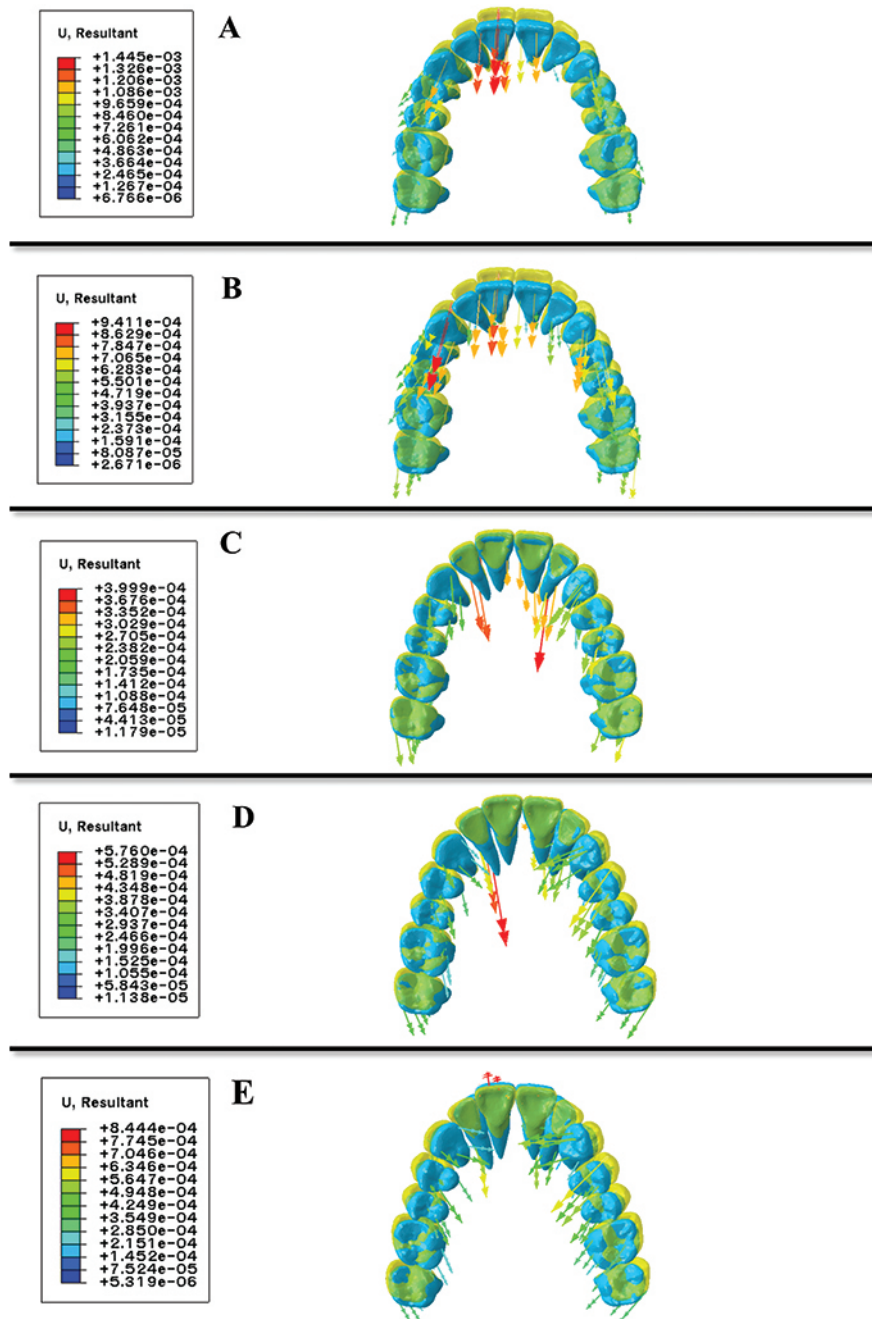


**Figure 6** Displacement of all maxillary teeth indicated by superimposition of before (yellow) and after (blue) application of the distalization force in the occlusal view. The direction of tooth movement indicated by the colored arrows. A) 0-mm, B) 2-mm, C) 4-mm, D) 6-mm, E) 8-mm lengths



and stress were also transferred to the second molar, causing posterior tooth movement and whole arch distalization. Thus, this finite element finding may be used as evidence to support the theory of en-masse distalization, which proposes that the entire maxillary dentition can be effectively moved after applying force to an anteriorly located hook.<sup>(24)</sup>

In this study, the results of stress distribution in the PDL were examined in terms of the von Mises stress. It was used to represent the overall stress of a multi-axial stress just the same as it has been applied in previous studies.<sup>(22,24,35-37)</sup> The stress on the teeth close to the point of force application at the retraction hook, was more concentrated than on some other teeth in positions farther from the hook. With 0-mm- and 2-mm- hooks, the highest level of stress was found at the cervical third of canine. With the other lengths, the highest level of stress was found on the apex of lateral incisor, which was also close to the point of force application. These outcomes are in agreement with those of Sung *et al.*<sup>(24)</sup>

The results revealed that the length of retraction hook highly relates to the types of tooth movement. Changing the length of retraction hook affects the distance between the line of action of force and the CRes. When distalization force is applied to low-level hooks, the line of action of the force passed below the CRes and induced clockwise moment, resulting in steepening of the occlusal plane. Consequently, the anterior teeth had palatal crown tipping and extrusion. The posterior teeth tipped distally and substantially intruded (Figure 7A). The level of stress was high at the distal root of the second molar because the posterior teeth were intruded. Moreover, the constructed tuberosity distal to the second molar and the boundary conditions at the back of the model may have strongly resisted the distalization, resulting in high stress in the distal root of the second molar (Figure 4A & B). On the other hand, the line of action of the force passed above the CRes and

generated counterclockwise moment, resulting in upward rotation of the occlusal plane. The labial flaring of anterior teeth was observed, and the posterior teeth were slightly extruded (Figure 7C). The stress in the PDL of posterior teeth was less than that with shorter hooks because extrusion occurred (Figure 4D & E).

When a distalization force was applied to a 4-mm hook, the line of action of the force passed near the CRes, rather than passing through it, and a low moment was generated. The line of force may have passed either slightly below or slightly above the CRes; therefore, the low moment may have been either clockwise or counterclockwise, respectively (Figure 7B). All maxillary teeth moved distally along the occlusal plane with minimal intrusion or tipping. The location of the miniscrew at the Modified IZC was higher than the CRes resulted in a distal and upward direction of the line of action of force, generating intrusion and distalization of the maxillary dentition. In whole arch distalization, the entire maxillary dentition did not undergo pure bodily movement. The reason may be archwire deflection of the force system, causing a relatively some degree of tipping movement.

All of the tooth displacement patterns studied correspond with the results of previous studies that used different lengths of retraction hook for whole arch distalization with interradicular miniscrews<sup>(24)</sup>, and for distalization of the posterior teeth with modified IZC miniscrews.<sup>(38)</sup>

The distalization force can be divided in to three axes which affect to the occurred displacement pattern. The amount of force in each axis was calculated and represented as  $F_x$ ,  $F_y$ , and  $F_z$ .  $F_x$  was a lateral force along the x axis;  $F_y$  was an intrusive force along the y axis;  $F_z$  was the horizontal force or distalization force along the z axis. These forces were calculated from the resultant force formula of three vectors using the angle values in this finite

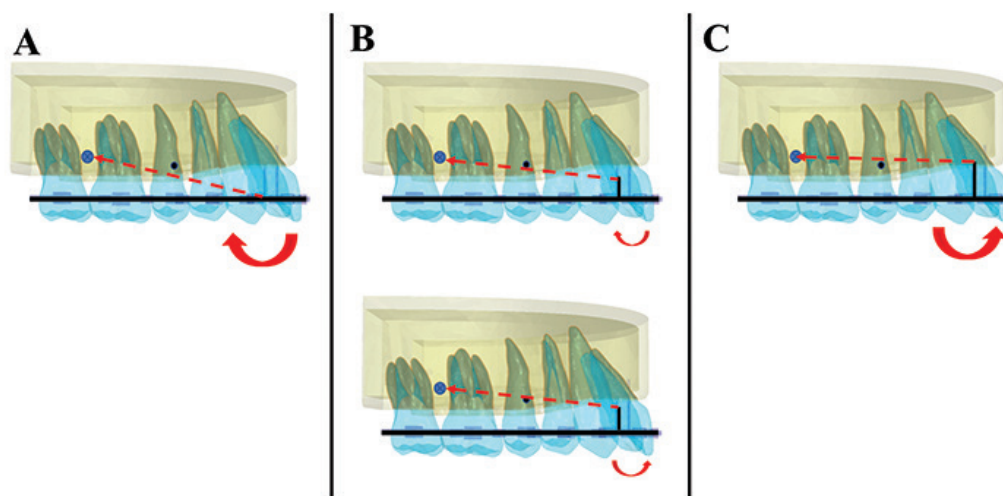


**Figure 7** Schematic diagram of moments on whole arch distalization using retraction hooks and miniscrews. A black dot indicates the position of the CRes. Red dotted lines indicate the distalization force. Red solid curved arrows express the moments that originated from the force. A) 0-mm hook (short): the red dotted line passes below the CRes, and a clockwise moment is generated. B) 4-mm hook: the red dotted line passes near the CRes, and a low moment is generated which may be clockwise or counterclockwise. C) 8-mm hook (long): the red dotted line passes above the CRes, and a counterclockwise moment is generated.

element model. The  $\theta$  angle was the angle formed between the line of action of force and the horizontal plane (Z-axis), whereas the  $\alpha$  angle was the angle formed between the line of action of force and the lateral force vector (X-axis), as shown in Figure 8. The  $\alpha$  angle varied, depending on the length of retraction hook. An increase in its length led to a decrease in the  $\theta$  angle. The  $\theta$  angle is zero when the level of the retraction hook is the same as that of the miniscrew.<sup>(39)</sup> In contrast, the  $\alpha$  angle value remained constant because the locations of retraction hook and miniscrew were fixed.

When using short hooks, the  $\theta$  angle becomes larger, resulting in high  $F_y$  (intrusive force) and low  $F_z$  (distalization force).<sup>(39)</sup> In our study, shorter hooks resulted in greater intrusion of the posterior teeth than did longer hooks. In contrast, long hooks the  $\theta$  angle was reduced, resulting in low  $F_y$  and high  $F_z$ . Therefore, the intrusion of posterior teeth was less than with shorter hooks.

Additionally, we found that the arch wire deflection occurred when using a retraction hook attached to the main archwire due to high bending moments at the joint of these two components. The high bending moments increase progressively according to the length of the retraction hook and the flexibility of the main archwire.<sup>(25)</sup> As found with high-level hooks, the anterior segment of the archwire was raised upward because a bending moment occurred between the lateral incisor and canine. Consequently, the deflection of archwire induced an intrusive force acting on the anterior teeth, thereby causing labial flaring of incisors. Additionally, the palatal crown tipping of the posterior teeth when using the high-level hooks gradually increased from a twist of the posterior segment of the archwire. This twist may have acted on the teeth in the same way as the third order bend or torque that occurs when archwires are bent using pliers. We attributed the deflection and flexibility of the archwire to the property of the

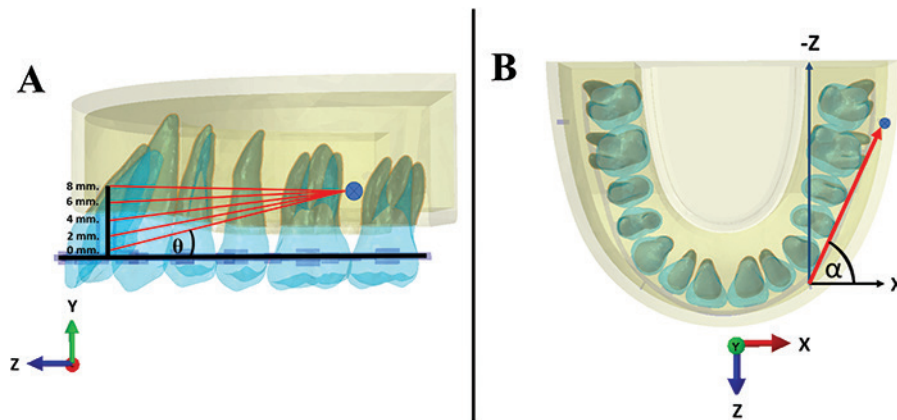


**Figure 8** Schematic force diagram and the angle of force in the horizontal and vertical planes. A) sagittal view of finite element model showing the  $\theta$  angle. B) top view of the model showing the  $\alpha$  angle

main archwire, which was assigned to be an elastic material because the idea of an orthodontic archwire with rigid strength is unrealistic.<sup>(24)</sup>

In this study, all materials were assigned as linear elastic properties, excepting the PDL, which was defined as having non-linear elasticity because of its hyper-elastic behavior. The Ogden model was used to express the elastic response of this biological soft tissues.<sup>(34)</sup> These material property values normally vary in each person owing to individual differences in histologic tissue properties.<sup>(20)</sup> Additionally, the thickness of PDL is, in fact, non-uniform, having an hour-glass shape with the mid-root level having the narrowest width;<sup>(40)</sup> however, in this study, it was assumed to be uniform (0.2 mm).

The selection of a hook length for whole arch distalization in each case should be based on the existing malocclusion and the specific treatment plan for each patient.<sup>(21,38)</sup> Short hooks could be effective for palatal crown tipping of the anterior teeth and intrusion of the posterior teeth which are suitable for the flared incisors and open bite case. Intrusion of the posterior teeth resulted in autorotation of mandibular and decreased the open bite. Long hooks should be used for palatal root movement of the anterior teeth and minor extrusion of the posterior teeth, resulting

in the posterior rotation of mandible. Thus, long hooks are suitable for the retroclined incisors and deep overbite case.<sup>(24)</sup>

The greater the concentration of stress, the larger is the hyalinized zone of PDL, resulting in a reduced rate of tooth movement and leading to root resorption.<sup>(41,42)</sup> Therefore, when applying whole arch distalization, the roots of the anterior teeth may be highly prone to resorption due to higher stress in those teeth.

Three-dimension computed tomography may be used in future studies to create individual tooth models for better simulations of orthodontic tooth movement and for greater accuracy in treatment planning.<sup>(20,21,38,43)</sup> Besides, studies can be improved by studying the duration of tooth movement. Treatment duration is an important factor that may yield different results from those of this static FEM study. Therefore, dynamic FEM studies may provide an increasingly realistic basis for orthodontic tooth movement.

## Conclusions

1. Different lengths of retraction hooks resulted in different patterns of stress distribution in the PDL and in different patterns of displacement of the

maxillary teeth in whole arch distalization.

- The von Mises stress in the PDL of the anterior teeth, especially the teeth near the retraction hook, was greater than in the PDL of the posterior teeth with all lengths of retraction hook. Areas of high stress concentration were also found in the intruded teeth, the second molar when using short hook and the anterior teeth for long hook.

- The use of short hooks induced palatal crown tipping with extrusion of the anterior teeth and distal crown tipping with intrusion of the posterior teeth. In contrast, the use of long hooks induced labial crown tipping with intrusion of the anterior teeth and distal crown tipping with extrusion of the posterior teeth.

2. The optimal length of retraction hook was 4 mm that produced movement closed to distal translation of the maxillary whole arch along the occlusal plane; however, pure bodily movement did not occur.

## Acknowledgments

The authors would like to acknowledge Mr. Pattarapon Saigerdsri, Master degree student, Faculty of Engineering, Chiang Mai University, Thailand for his assistance in the use of the SolidWorks and Abaqus software during the research study, and Dr. M. Kevin O. Carroll, Professor Emeritus of the University of Mississippi School of Dentistry, USA and Faculty Consultant at Faculty of Dentistry, Chiang Mai University Thailand, for language editing.

## References

1. Park HS, Kwon TG, Sung JH. Nonextraction treatment with micro screw implants. *Angle Orthod* 2004; 74(4): 539-549.
2. Janson G, Barros SEC, Simão TM, Freitas MRD. Relevant variables of Class II malocclusion treatment. *Dental Press J Orthod* 2009; 14(4): 149-157.
3. Burstone CJ, Choy K. *The biomechanical foundation of clinical orthodontics*. Hanover Park: Quintessence Publishing; 2015: 580.
4. Proffit WR, Fields HW, Sarver DM. Mechanical principles in orthodontic force control. *Contemporary orthodontics*. 5<sup>th</sup> ed. St.Louis: Mosby Elsevier; 2013: 312-336.
5. Chen G, Teng F, Xu TM. Distalization of the maxillary and mandibular dentitions with miniscrew anchorage in a patient with moderate Class I bimaxillary dentoalveolar protrusion. *Am J Orthod Dentofacial Orthop* 2016; 149(3): 401-410.
6. Choi YJ, Lee JS, Cha JY, Park YC. Total distalization of the maxillary arch in a patient with skeletal Class II malocclusion. *Am J Orthod Dentofacial Orthop* 2011; 139(6): 823-833.
7. Lee KJ, Park JY, Park YC. En-masse distalization of upper dentition for correction of Class II using dual orthodontic miniscrews. *J Dent Assoc Thai* 2006; 5: 33-38.
8. Wu X, Liu H, Luo C, Li Y, Ding Y. Three-dimensional evaluation on the effect of maxillary dentition distalization with miniscrews implanted in the infrazygomatic crest. *Int J Implant Dent* 2017; 27(1): 22-27.
9. Liu H, Wu X, Yang L, Ding Y. Safe zones for miniscrews in maxillary dentition distalization assessed with cone-beam computed tomography. *Am J Orthod Dentofacial Orthop* 2017; 151(3): 500-506.
10. Fayed MM, Pazera P, Katsaros C. Optimal sites for orthodontic mini-implant placement assessed by cone beam computed tomography. *Angle Orthod* 2010; 80(5): 939-951.
11. Noorollahian S, Alavi S, Shirban F. Bilateral en-masse distalization of maxillary posterior teeth with skeletal anchorage: a case report. *Dental Press J Orthod* 2016; 21(3): 85-93.

12. Lin JJJ. New method of distalization of the maxillary dentition using the infrazygomatic crest mini-screws. *Creative orthodontics: blending the Damon system and TADs to manage difficult malocclusions*. 2<sup>nd</sup> ed. Taipei: Yong Chieh Enterprise 2010: 187-208.
13. Lin JJJ, Roberts. Guided infrazygomatic screws: reliable maxillary arch retraction. *Int J Orthod Implantol* 2017; 46: 4-16.
14. Bechtold TE, Kim JW, Choi TH, Park YC, Lee KJ. Distalization pattern of the maxillary arch depending on the number of orthodontic miniscrews. *Angle Orthod* 2013; 83(2): 266-273.
15. Tekale PD, Vakil KK, Vakil JK, Gore KA. Distalization of maxillary arch and correction of Class II with mini-implants: A report of two cases. *Contemp Clin Dent* 2015; 6(2): 226.
16. Nanda RS, Tosun YS. *Biomechanics in orthodontics principle and practice*. 1<sup>st</sup> ed. Hanover Park: Quintessence Publishing; 2010: 1-145.
17. Knop L, Gandini LG, Shintcovsk RL, Gandini MR. Scientific use of the finite element method in orthodontics. *Dental Press J Orthod* 2015; 20(2): 119-125.
18. Marya A, David G, Eugenio MA. Finite element analysis and its role in orthodontics. *Dent Oral Health* 2016; 2(2): 5-6.
19. Konda P, Tarannum S. Basic principles of finite element method and its applications in orthodontics. *J Pharm Biomed Sci* 2012; 16(16): 1-8.
20. Cho SM, Choi SH, Sung SJ, Yu HS, Hwang CJ. The effects of alveolar bone loss and miniscrew position on initial tooth displacement during intrusion of the maxillary anterior teeth: finite element analysis. *Korean J Orthod* 2016; 46(5): 310-322.
21. Mo SS, Kim SH, Sung SJ, et al. Factors controlling anterior torque with C-implants depend on en-masse retraction without posterior appliances: biocreative therapy type II technique. *Am J Orthod Dentofacial Orthop* 2011; 139(2): 183-191.
22. Seong EH, Choi SH, Kim HJ, Yu HS, Park YC, Lee KJ. Evaluation of the effects of miniscrew incorporation in palatal expanders for young adults using finite element analysis. *Korean J Orthod* 2018; 48(2): 81-89.
23. Song JW, Lim JK, Lee KJ, Sung SJ, Chun YS, Mo SS. Finite element analysis of maxillary incisor displacement during en-masse retraction according to orthodontic mini-implant position. *Korean J Orthod* 2016; 46(4): 242- 52.
24. Sung EH, Kim SJ, Chun YS, Park YC, Yu HS, Lee KJ. Distalization pattern of whole maxillary dentition according to force application points. *Korean J Orthod* 2015; 45(1): 20-28.
25. Sang SJ, Jang GW, Chun YS, Moon YS. Effective en-masse retraction design with orthodontic mini-implant anchorage: a finite element analysis. *Am J Orthod Dentofacial Orthop* 2010; 137(5): 648-657.
26. Hemanth M, Lodaya SD. Orthodontic force distribution: a three-dimensional finite element analysis. *World J Dent* 2010; 1(3): 159-162.
27. Mohammed SD, Desai H. Basic concepts of finite element analysis and its applications in dentistry: an overview. *J Oral Hyg Health* 2014; 2(5): 156-160.
28. Desai SR, Harshada SH. Finite element analysis: basics and its applications in dentistry. *Indian J Dent Sci* 2012; 4(1): 60-65.
29. Geramy A, Sodagar A, Hassanpour M. Three-dimensional analysis using finite element method of anterior teeth inclination and center of resistance location. *Chin J Dent Res* 2014; 1: 37-42.

30. Jagota V, Sethi APS, Kumar K. Finite element method: An overview. *Walailak J Sci & Tech* 2013; 10(1): 1-8.
31. Jeong GM, Sung SJ, Lee KJ, Chun YS, Mo SS. Finite-element investigation of the center of resistance of the maxillary dentition. *Korean J Orthod* 2009; 39(2): 83-94.
32. Toms SR, Eberhardt AW. A nonlinear finite element analysis of the periodontal ligament under orthodontic tooth loading. *Am J Orthod Dentofacial Orthop* 2003; 123(6): 657-665.
33. Tanne K, Sakuda M, Burstone CJ. Three-dimensional finite element analysis for stress in the periodontal tissue by orthodontic forces. *Am J Orthod Dentofacial Orthop* 1987; 92(6): 499-505.
34. Huang H, Tang W, Yan B, Wu B. Mechanical responses of periodontal ligament under a realistic orthodontic loading. *Procedia Eng* 2012; 31: 828-833.
35. Jing Y, Han X, Cheng B, Bai D. Three-dimensional FEM analysis of stress distribution in dynamic maxillary canine movement. *Chinese Science Bulletin* 2013; 58(20): 2454-2459.
36. Yu IJ, Kook YA, Sung SJ, Lee KJ, Chun YS, Mo SS. Comparison of tooth displacement between buccal mini-implants and palatal plate anchorage for molar distalization: a finite element study. *Eur J Orthod* 2014; 36(4): 394-402.
37. Chen YC, Tsai HH. Use of 3D finite element models to analyze the influence of alveolar bone height on tooth mobility and stress distribution. *J Dent Sci* 2011; 6(2): 90-94.
38. Aungkatawiwat T, Patanaporn V, Rungsiyakull C. Maxillary posterior teeth distalization with miniscrew anchorage relative to force vectors applied to different lengths of retraction hook, analyzed using the finite element method. *CM Dent J* 2018; 39(2): 77-89.
39. Meriam JL, Kraige LG. *Engineering Mechanics: Statics* 7<sup>th</sup> ed. New York: John Wiley & Sons, Inc.; 2004: 523.
40. Anthony P. The anatomy and physiology of the healthy periodontium. In: Panagakos F, editor. *Gingival diseases - Their aetiology, prevention and treatment*. Rijeka: InTech; 2011: 1-22.
41. Tomizuka R, Shimizu Y, Kanetaka H, et al. Histological evaluation of the effects of initially light and gradually increasing force on orthodontic tooth movement. *Angle Orthod* 2007; 77(3): 410-416.
42. Böhl MV, Jagtman AMK. Hyalinization during orthodontic tooth movement: a systematic review on tissue reactions. *Eur J Orthod* 2009; 31(1): 30-36.
43. Tajima K, Chen KK, Takahashi N, Noda N, Nagamatsu Y, Kakigawa H. Three-dimensional finite element modeling from CT images of tooth and its validation. *Dent Mater J* 2009; 28(2): 219-226.